ACS APPLIED MATERIALS & INTERFACES

Research Article

www.acsami.org

Bioinspired Ternary Artificial Nacre Nanocomposites Based on Reduced Graphene Oxide and Nanofibrillar Cellulose

Jianli Duan,[†,∥] Shanshan Gong,[†,∥] Yuan Gao,[†,∥] Xiaolin Xie,[§] Lei Jiang,[†] and Qunfeng Cheng*[,†,‡]

[†]Key Laboratory of Bio-inspired Smart Interfacial Science and Technology of Ministry of Education, School of Chemistry and Environment, BeiHang University, Beijing 100191, China

[‡]State Key Laboratory for Modification of Chemical Fibers and Polymer Materials, Donghua University, Shanghai 201620, China

[§]Key Laboratory for Material Chemistry of Energy Conversion and Storage, Ministry of Education, School of Chemistry and Chemical Engineering, Huazhong University of Science and Technology, Wuhan 430074, China

Supporting Information

ABSTRACT: Inspired by the nacre, we demonstrated the integrated ternary artificial nacre nanocomposites through synergistic toughening of graphene oxide (GO) and nanofibrillar cellulose (NFC). In addition, the covalent bonding was introduced between adjacent GO nanosheets. The synergistic toughening effects from building blocks of one-dimensional NFC and two-dimensional GO, interface interactions of hydrogen and covalent bonding together result in the integrated mechanical properties including high tensile strength, toughness, and fatigue life as well as high electrical conductivity. These extraordinary properties of the ternary synthetic nacre nanocomposites allow the support for advances in diverse strategic fields including stretchable electronics, transportation, and energy. Such bioinspired strategy also provides a new insight in designing novel multifunctional nanocomposites.

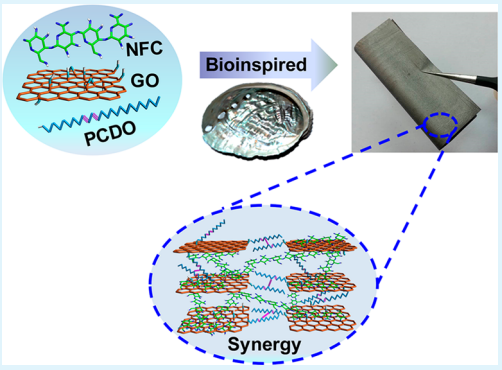

KEYWORDS: *bioinspired, ternary artificial nacre, graphene oxide, nanofibrillar cellulose, mechanical properties*

INTRODUCTION

Over the course of time, billions of years in fact, nacre has achieved outstanding mechanical properties by constructing hierarchical micro/nanoscale structure, with abundant interface interactions and synergistic effects.[1] Nacre is essentially laminated composite containing alternately hexagonal platelets of aragonite cross-linked with a thin layer of organic material, including nanofibrillar chitin[2] and softer protein.[3,4] The intrinsic structure and synergistic effects of nacre inspired many researchers to build ternary artificial nacre through assembling two-dimensional (2D) and one-dimensional (1D) building blocks with cross-linking of organic molecules, which plays a key role in fabricating high-performance nanocomposites. Prasad et al.[5] demonstrated such synergistic effect by using two different nanocarbons (graphene nanosheets and single-walled carbon nanotube (SWNT)) with the matrix of poly(vinyl alcohol) (PVA). Shin et al.[6] also demonstrated super tough ternary nanocomposite fibers via synergistic building blocks of reduced GO (rGO) and SWNT in the matrix of PVA. We have also built ternary nanocomposites with excellent mechanical performance through synergistic effect from 1D and 2D building blocks, such as nanoclay-nanofibrillar cellulose (NFC)-PVA,[7] and rGO/molybdenum disulfide (MoS_2)/thermoplastic polyurethanes (TPU) (rGO-MoS2-TPU).[8] Recently, we constructed GO-based nanocomposites through synergistic toughening, indicating outstanding mechanical properties.[9] Despite these advances, fundamental basic research regarding the design and fabrication of ternary nacre-like nanocomposites using synergistic toughening of building blocks plus interface interactions is still needed.

In this study, NFC was chosen as 1D building block. The NFC is inexpensive, ecofriendly, and easy to obtain as compared with double-walled carbon nanotube (DWNT).[9] The NFC, mainly derived from wood with diameter in the nanoscale and length in the microscale,[10,11] shows high elastic modulus of ∼150 GPa[12] and abundant hydroxyl groups on its surface,[13] thus suitable for constructing interface interactions with GO sheets via hydrogen bonding network. Herein, we demonstrated an integrated artificial nacre-like nanocomposite through synergistic toughening of 1D NFC and 2D GO sheets as building blocks and covalently cross-linking. This kind of ternary artificial nacre nanocomposite shows the ultimate stress of 314.6 MPa and a toughness of 9.8 MJ/m^3. Meanwhile, the ternary artificial nacre also demonstrates high fatigue life and electrical conductivity as high as 162.6 S/cm. This kind of high-performance artificial nacre supports advances in diverse strategic fields including nanomembrane sensors, stretchable electronics, transportation, and/or energy. Such bioinspired

Received: February 21, 2016
Accepted: April 7, 2016
Published: April 7, 2016

DOI: 10.1021/acsami.6b02156
ACS Appl. Mater. Interfaces 2016, 8, 10545−10550

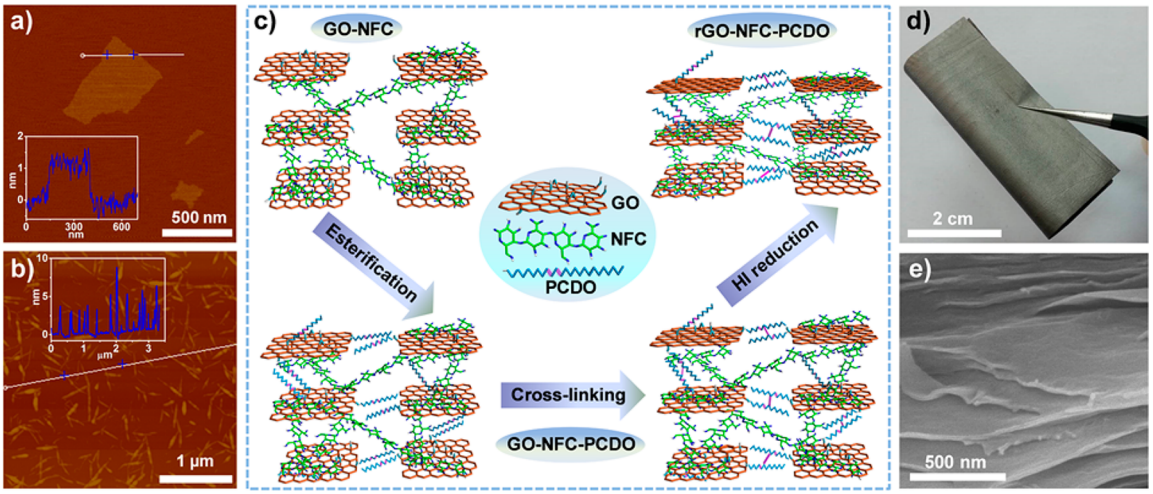

Figure 1. Size of GO nanosheets (a) and rodlike NFC fibrils (b). (c) Schematic illustration of fabrication procedure of ternary artificial nacre nanocomposites. A digital image (d) and the cross-section morphology (e) of ternary artificial nacre nanocomposites.

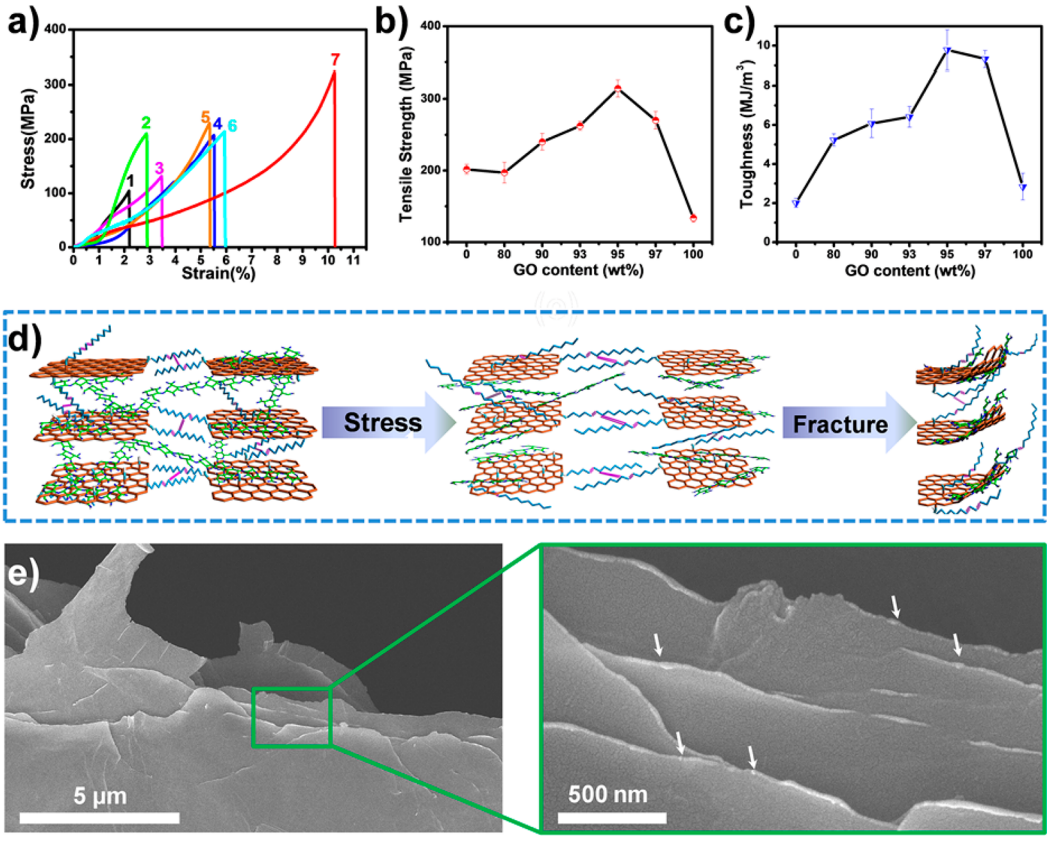

Figure 2. (a) Typical stress−strain curves of GO film (Curve 1), NFC film (Curve 2), rGO film (Curve 3), GO-NFC-IV hybrid materials (Curve 4), GO-NFC-PCDO-IV nanocomposites (Curve 5), rGO-NFC-IV hybrid materials (Curve 6), and rGO-NFC-PCDO-IV nanocomposites (Curve 7). (b, c) The mechanical properties of rGO-NFC-PCDO nanocomposites with different GO loading. (d) The proposed fracture mechanism of rGO-NFC-PCDO-IV ternary artificial nacre nanocomposite under stress. (e) The side view of rGO-NFC-PCDO-IV nanocomposites after tensile testing.

strategy using synergistic toughening mechanisms also provides new vision for designing novel multifunctional nanocomposites. The Experimental Section is listed in the Supporting Information.

■ RESULTS AND DISCUSSION

GO nanosheets prepared using modified Hummers' method had the size in a range of 0.2−0.7 μm and the thickness of ∼1.0 nm (Figure 1a). NFC fibrils were prepared based on the previous reports.[13,14] NFC fibrils show the length of 200−800 nm and average diameter of ∼4.1 nm (Figure 1b). Nacre-like nanocomposites were constructed using the technique shown in Figure 1c. First, binary GO-NFC layered nanocomposites were assembled via evaporation process. Five kinds of GO-NFC binary nanocomposites with ratios of (GO/NFC = 80:20, 90:10, 93:7, 95:5, 97:3) were fabricated and listed as GO-NFC-I, GO-NFC-II, GO-NFC-III, GO-NFC-IV, and GO-NFC-V,

DOI: 10.1021/acsami.6b02156
ACS Appl. Mater. Interfaces 2016, 8, 10545−10550

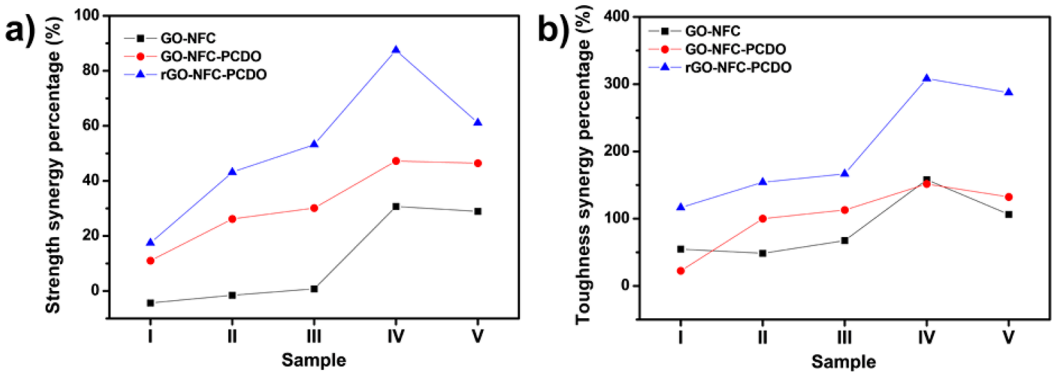

Figure 3. Synergy percentage of increases with GO contents in binary GO-NFC hybrid layered materials, GO-NFC-PCDO, and rGO-NFC-PCDO ternary artificial nacre nanocomposites: (a) strength and (b) toughness synergy percentage.

respectively. The exact content of GO in the binary-layered nanocomposites was determined by TGA (Supporting Information, Figure S1 and Table S1). Next the GO-NFC binary-layered nanocomposites were covalently cross-linked through 10,12-pentacosadiyn-1-ol (PCDO) according to the previous report,[15] resulting in the GO-NFC-PCDO ternary nacre-like nanocomposites. After chemical reduction with hydroiodic acid (HI), the obtained rGO-NFC-PCDO ternary artificial nacre nanocomposites (Figure 1d) show the layered structure (Figure 1e).

X-ray diffraction (XRD) results confirmed that NFC and PCDO were successfully introduced into the interlayers of the GO nanosheets (Supporting Information, Figure S2 and Table S2). As NFC was added, the *d*-spacing of GO-NFC increased, indicating that NFC was uniformly distributed in the interlayer of GO-NFC binary layered nanocomposites. After grafting with PCDO molecules, the *d*-spacing of GO-NFC-PCDO nanocomposites further increased. On the contrary, the *d*-spacing of rGO-NFC-PCDO nacre-like nanocomposites notably decreased.[15] Fourier transform infrared spectroscopy (FTIR) and X-ray photoelectron spectra (XPS) are also conducted to verify the covalent cross-linking by PCDO molecules,[16,17] as shown in Figures S3 and S4 (Supporting Information).

As shown in Figure 2a, the pure GO film exhibits the tensile strength of 104.7 ± 1.4 MPa and toughness of 1.1 ± 0.2 MJ/m^3 (Curve 1 in Figure 2a). The pure NFC film shows high mechanical properties with tensile strength of 201.8 ± 6.8 MPa and toughness of 2.0 ± 0.2 MJ/m^3 (Curve 2 in Figure 2a). After reduction by HI, rGO film indicates the ultimate strength of 133.7 ± 5.8 MPa and toughness of 2.8 ± 0.7 MJ/m^3 (Curve 3 in Figure 2a). For the GO-NFC films with different loadings of GO, the optimized maximum mechanical properties are realized at the GO loading of 94.7 wt % (GO-NFC-IV; Supporting Information, Figure S5), and listed in Table S3 (Supporting Information). The GO-NFC-IV reach tensile strength of 200.3 ± 6.7 MPa and toughness of 4.0 ± 0.2 MJ/m^3 (Curve 4 in Figure 2a). The mechanical properties of GO-NFC-PCDO-IV nanocomposites with covalent cross-linking by PCDO are enhanced to 225.6 ± 4.1 MPa and 3.9 ± 0.2 MJ/m^3 (Curve 5 in Figure 2a). The PCDO content is ~2.82 wt %, as determined by TGA, shown in Figure S6 (Supporting Information). The mechanical properties of rGO-NFC-IV and rGO-NFC-PCDO-IV nanocomposites are improved to 214.8 ± 7.8 MPa and 5.2 ± 0.5 MJ/m^3 (Curve 6 in Figure 2a) and to 314.6 ± 11.7 MPa and 9.8 ± 1.0 MJ/m^3 (Curve 7 in Figure 2a), respectively. Figure 2b,c shows the trend of mechanical properties of rGO-NFC-PCDO nanocomposites with different GO loading. The mechanical properties of rGO-NFC-PCDO-IV with GO content of 94.7 wt % especially demonstrate the maximum values, consistent with natural nacre having almost 95 vol % inorganic aragonite and also consistent with the idea of biomimetic concept.[1]

The proposed fracture mechanism of our nacre-like nanocomposites is shown in Figure 2d. First, the hydrogen bonding between rGO and NFC is destroyed, accompanying with the slippage between adjacent rGO nanosheets and the NFC to resist the sliding, resulting in the stress uniformly dispersed in the rGO nanosheets and NFC. Meanwhile, much more energy is dissipated in the process of stretching PCDO molecules.[15] The NFC chains are also pulled out after further stretching process. Further loading results in the breaking of covalent cross-linking between PCDO and rGO nanosheets and curved edges of rGO nanosheets (Figures 2e). It is clearly shown that the GO nanosheets curved in rGO-NFC-PCDO nanocomposites and that the NFC was pulled out, as indicated with direction of arrows. With the increase of NFC contents in GO-NFC, more rodlike fibrils were distributed uniformly along the GO nanosheets. After cross-linking of PCDO and chemical reduction by HI, rGO nanosheets stacked closer, and rodlike fibrils were oriented along the direction of curved rGO nanosheets (Supporting Information, Figure S7).

The synergistic effect of the building blocks of GO nanosheets and NFC on the improvement of mechanical properties can be quantified using the synergy percentage (S),[5] which we modified as follows:

$$S = \frac{2M_{hyb} - (M_{NFC} + M_{GO})}{M_{NFC} + M_{GO}} \times 100$$

where M_{NFC}, M_{GO}, and M_{hyb} represent the mechanical properties of NFC film, GO film, and GO-NFC hybrid layered materials. The synergy percentage of GO-NFC and rGO-NFC-PCDO nanocomposites are also calculated (Supporting Information, Table S3). The strength synergy percentage increases with increasing GO content and reaches the maximum value of 30.7% for GO-NFC-IV when the GO content is 94.7 wt % (Figure 3a). Meanwhile, the toughness synergy percentage also reaches the maximum value of 158.1% for GO-NFC-IV (Figure 3b), indicating that synergistic effects can be optimized by adjusting the ratios of 1D NFC and 2D GO nanosheets, consistent with the previous report.[6] Furthermore, the synergy percentage can be further enhanced via strong interface interactions of covalently cross-linking.[9] The synergy percentage of strength and toughness increases to

DOI: 10.1021/acsami.6b02156
ACS Appl. Mater. Interfaces 2016, 8, 10545−10550

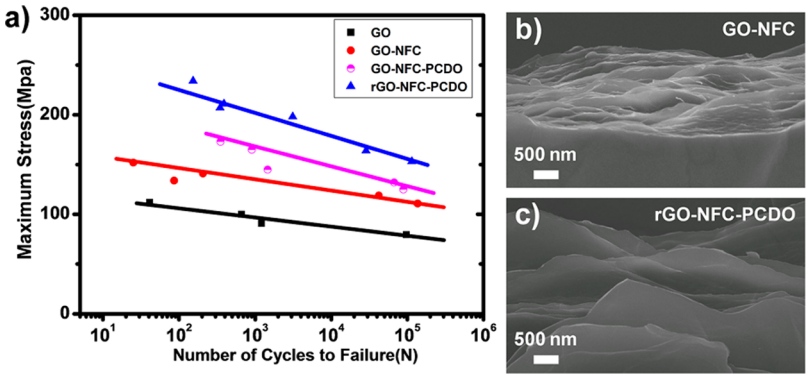

Figure 4. (a) Tensile fatigue testing of GO film, GO-NFC-IV hybrid layered materials, GO-NFC-PCDO-IV nanocomposites, and rGO-NFC-PCDO-IV ternary artificial nacre nanocomposites. (b) The fracture morphology of GO-NFC-IV hybrid layered materials and (c) rGO-NFC-PCDO-IV nanocomposite after fatigue testing.

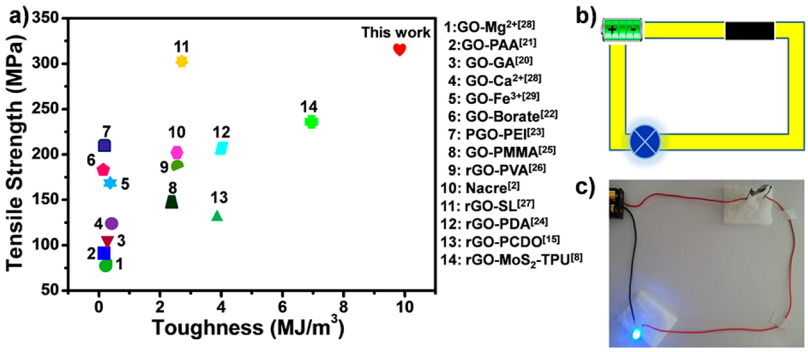

Figure 5. (a) Mechanical properties comparison. (b) Schematic of the circuit. (c) The digital photo of circuit.

87.5% and 308.3% for rGO-NFC-PCDO-IV nanocomposites, respectively. Compared with our previous work,[9] this study further confirms that the synergy percentage can be additionally improved via constructing hydrogen and covalent bonding together, which also provides a new strategy for improving the mechanical properties of layered nanocomposites.

This kind of synergistic effects from interface interactions and building blocks not only enhances the static mechanical properties of bioinspired nanocomposites but also dramatically improves the dynamic mechanical properties, such as the fatigue life. Herein, the cyclic tensile tests were performed to verify the fatigue life (Figure 4a),[18] and the corresponding stress−strain fatigue curves are listed in Figure S8 (Supporting Information). The fatigue life of rGO-NFC-PCDO nanocomposites is much higher than that of GO-NFC hybrid layered materials and GO-NFC-PCDO-IV nanocomposites at the same stress level, which indicates the synergistic toughening effects from building blocks of GO, NFC, and interfacial interactions together. The fracture morphology of GO-NFC hybrid layered materials and rGO-NFC-PCDO nacre-like nanocomposites were investigated by SEM (Figure 4b,c). The crack propagation was suppressed by GO nanosheets by crack deflection. The covalent bonding between adjacent 2D rGO nanosheets in the rGO-NFC-PCDO-IV ternary artificial nacre nanocomposites also plays a key role in suppressing crack propagation via crack bridging and a subsequent broken of covalent bonding, resulting in curving of rGO nanosheets (Figure 4c). The fatigue life is prolonged through crack deflection and bridging together.

Figure 5a indicates that the integrated mechanical properties of rGO-NFC-PCDO nanocomposites are higher than nacre[2] and other GO-based nanocomposites.[19] For example, the GO nanosheets are covalently cross-linked with different molecules, such as glutaraldehyde (GO-GA),[20] polyallylamine (GO-PAA),[21] borate (GO-borate),[22] poly(ether imide) (PGO−PEI),[23] 10,12-pentacosadiyn-1-ol (rGO-PCDO),[15] and poly(dopamine) (rGO-PDA).[24] In addition, the GO-based nanocomposites with other interfacial interactions also show lower mechanical properties than this kind of ternary artificial nacre nanocomposites, including hydrogen bonding with poly(methyl methacrylate) (GO-PMMA),[25] poly(vinyl alcohol) (rGO-PVA),[26] silk (rGO-SL),[27] and ionic bonding with calcium (GO-Ca^{2+}),[28] magnesium (GO-Mg^{2+}),[28] and iron (GO-Fe^{3+}).[29] Table S5 (Supporting Information) listed the corresponding tensile strength and toughness.

Furthermore, the electrical conductivity of the rGO-NFC-PCDO-V nanocomposites with 162.6 S/cm is higher than that of previous rGO-MoS_2-TPU,[8] rGO-PCDO[15] nanocomposites, and the other cellulose nanocrystals/rGO nanocomposites.[30] Building a circuit, using the blue LED bulb connected to the power supply, and using the nanocomposite as a conducting wire, the electrical conductivity of the rGO-NFC-PCDO ternary nacre-like nanocomposites was investigated. The test shows excellent conductivity of the nanocomposite wire. The nacre-like nanocomposites can also be easily folded without breaking (Figure 5b,c), indicating their applicability in flexible and stretchable electronic devices.

■ CONCLUSION

Nature is far more successful in designing strong and tough materials than with most man-made materials and provides an inspiration for designing novel nanocomposites. Using nacre as

DOI: 10.1021/acsami.6b02156
ACS Appl. Mater. Interfaces 2016, 8, 10545−10550

an example, we have successfully constructed integrated ternary artificial nacre-like nanocomposites through synergistic toughening of graphene oxide nanosheets and nanofibrillar cellulose. The synergistic toughening effects of building blocks and interface interactions resulted in outstanding integrated mechanical properties, as well as high electrical conductivity and excellent fatigue properties. These outstanding properties provide promising applications in the fields of stretchable electronics, transportation, and energy. Such bioinspired strategy also provides a new insight and clever guidelines in designing novel multifunctional nanocomposites.

■ ASSOCIATED CONTENT

Supporting Information

The Supporting Information is available free of charge on the ACS Publications website at DOI: 10.1021/acsami.6b02156.

Experimental materials, preparation of GO-NFC hybrid materials, preparation of nanocomposites, characterization, TGA curves, XRD, XPS, and FTIR spectra, stress and toughness measurements, fracture morphology, stress−strain fatigue curves, d-spacing of nanocomposites, electrical and mechanical properties of rGO film and nanocomposites, additional references. (PDF)

■ AUTHOR INFORMATION

Corresponding Author

*E-mail: cheng@buaa.edu.cn.

Author Contributions

‖J.D., S.G., and Y.G. contributed equally to this work.

Notes

The authors declare no competing financial interest.

■ ACKNOWLEDGMENTS

This work was supported by the Excellent Young Scientist Foundation of NSFC (51522301), the National Natural Science Foundation of China (21273017, 51103004), the Program for New Century Excellent Talents in University (NCET-12-0034), the Beijing Nova Program (Z121103002512020), the Fok Ying-Tong Education Foundation (141045), the Open Project of Beijing National Laboratory for Molecular Sciences, the 111 Project (B14009), the Aeronautical Science Foundation of China (20145251035, 2015ZF21009), the State Key Laboratory for Modification of Chemical Fibers and Polymer Materials, Donghua University (LK1508), the Key Research Program of the Chinese Academy of Sciences (KJZD-EW-M03), and the Fundamental Research Funds for the Central Universities (YWF-15-HHXY-001).

■ REFERENCES

(1) Wegst, U. G.; Bai, H.; Saiz, E.; Tomsia, A. P.; Ritchie, R. O. Bioinspired Structural Materials. *Nat. Mater.* **2014**, *14*, 23−36.

(2) Meyers, M. A.; McKittrick, J.; Chen, P.-Y. Structural Biological Materials: Critical Mechanics-Materials Connections. *Science* **2013**, *339*, 773−779.

(3) Suzuki, M.; Saruwatari, K.; Kogure, T.; Yamamoto, Y.; Nishimura, T.; Kato, T.; Nagasawa, H. An Acidic Matrix Protein, Pif, Is a Key Macromolecule for Nacre Formation. *Science* **2009**, *325*, 1388−1390.

(4) Laaksonen, P.; Walther, A.; Malho, J. M.; Kainlauri, M.; Ikkala, O.; Linder, M. B. Genetic Engineering of Biomimetic Nanocomposites: Diblock Proteins, Graphene, and Nanofibrillated Cellulose. *Angew. Chem., Int. Ed.* **2011**, *50*, 8688−8691.

(5) Prasad, K. E.; Das, B.; Maitra, U.; Ramamurty, U.; Rao, C. Extraordinary Synergy in the Mechanical Properties of Polymer Matrix Composites Reinforced with 2 Nanocarbons. *Proc. Natl. Acad. Sci. U. S. A.* **2009**, *106*, 13186−13189.

(6) Shin, M. K.; Lee, B.; Kim, S. H.; Lee, J. A.; Spinks, G. M.; Gambhir, S.; Wallace, G. G.; Kozlov, M. E.; Baughman, R. H.; Kim, S. J. Synergistic Toughening of Composite Fibres by Self-Alignment of Reduced Graphene Oxide and Carbon Nanotubes. *Nat. Commun.* **2012**, *3*, 650.

(7) Wang, J.; Cheng, Q.; Lin, L.; Jiang, L. Synergistic Toughening of Bioinspired Poly (Vinyl Alcohol)-Clay-Nanofibrillar Cellulose Artificial Nacre. *ACS Nano* **2014**, *8*, 2739−2745.

(8) Wan, S.; Li, Y.; Peng, J.; Hu, H.; Cheng, Q.; Jiang, L. Synergistic Toughening of Graphene Oxide-Molybdenum Disulfide-Thermoplastic Polyurethane Ternary Artificial Nacre. *ACS Nano* **2015**, *9*, 708−714.

(9) Gong, S.; Cui, W.; Zhang, Q.; Cao, A.; Jiang, L.; Cheng, Q. Integrated Ternary Bioinspired Nanocomposites *via* Synergistic Toughening of Reduced Graphene Oxide and Double-Walled Carbon Nanotubes. *ACS Nano* **2015**, *9*, 11568−11573.

(10) Klemm, D.; Kramer, F.; Moritz, S.; Lindström, T.; Ankerfors, M.; Gray, D.; Dorris, A. Nanocelluloses: A New Family of Nature-Based Materials. *Angew. Chem., Int. Ed.* **2011**, *50*, 5438−5466.

(11) Tingaut, P.; Zimmermann, T.; Sèbe, G. Cellulose Nanocrystals and Microfibrillated Cellulose as Building Blocks for the Design of Hierarchical Functional Materials. *J. Mater. Chem.* **2012**, *22*, 20105−20111.

(12) Iwamoto, S.; Kai, W.; Isogai, A.; Iwata, T. Elastic Modulus of Single Cellulose Microfibrils from Tunicate Measured by Atomic Force Microscopy. *Biomacromolecules* **2009**, *10*, 2571−2576.

(13) Okita, Y.; Saito, T.; Isogai, A. Entire Surface Oxidation of Various Cellulose Microfibrils by TEMPO-Mediated Oxidation. *Biomacromolecules* **2010**, *11*, 1696−1700.

(14) Saito, T.; Kimura, S.; Nishiyama, Y.; Isogai, A. Cellulose Nanofibers Prepared by TEMPO-Mediated Oxidation of Native Cellulose. *Biomacromolecules* **2007**, *8*, 2485−2491.

(15) Cheng, Q.; Wu, M.; Li, M.; Jiang, L.; Tang, Z. Ultratough Artificial Nacre Based on Conjugated Cross-Linked Graphene Oxide. *Angew. Chem.* **2013**, *125*, 3838−3843.

(16) Sukhishvili, S. A.; Granick, S. Layered, Erasable Polymer Multilayers Formed by Hydrogen-Bonded Sequential Self-Assembly. *Macromolecules* **2002**, *35*, 301−310.

(17) Xiong, R.; Hu, K.; Grant, A. M.; Ma, R.; Xu, W.; Lu, C.; Zhang, X.; Tsukruk, V. V. Ultrarobust Transparent Cellulose Nanocrystal-Graphene Membranes with High Electrical Conductivity. *Adv. Mater.* **2016**, *28*, 1501−1509.

(18) Yavari, F.; Rafiee, M.; Rafiee, J.; Yu, Z.-Z.; Koratkar, N. Dramatic Increase in Fatigue Life in Hierarchical Graphene Composites. *ACS Appl. Mater. Interfaces* **2010**, *2*, 2738−2743.

(19) Cheng, Q.; Jiang, L.; Tang, Z. Bioinspired Layered Materials with Superior Mechanical Performance. *Acc. Chem. Res.* **2014**, *47*, 1256−1266.

(20) Gao, Y.; Liu, L.-Q.; Zu, S.-Z.; Peng, K.; Zhou, D.; Han, B.-H.; Zhang, Z. The Effect of Interlayer Adhesion on the Mechanical Behaviors of Macroscopic Graphene Oxide Papers. *ACS Nano* **2011**, *5*, 2134−2141.

(21) Park, S.; Dikin, D. A.; Nguyen, S. T.; Ruoff, R. S. Graphene Oxide Sheets Chemically Cross-Linked by Polyallylamine. *J. Phys. Chem. C* **2009**, *113*, 15801−15804.

(22) An, Z.; Compton, O. C.; Putz, K. W.; Brinson, L. C.; Nguyen, S. T. Bio-Inspired Borate Cross-Linking in Ultra-Stiff Graphene Oxide Thin Films. *Adv. Mater.* **2011**, *23*, 3842−3846.

(23) Tian, Y.; Cao, Y.; Wang, Y.; Yang, W.; Feng, J. Realizing Ultrahigh Modulus and High Strength of Macroscopic Graphene Oxide Papers through Crosslinking of Mussel-Inspired Polymers. *Adv. Mater.* **2013**, *25*, 2980−2983.

(24) Cui, W.; Li, M.; Liu, J.; Wang, B.; Zhang, C.; Jiang, L.; Cheng, Q. A Strong Integrated Strength and Toughness Artificial Nacre Based on Dopamine Cross-Linked Graphene Oxide. *ACS Nano* **2014**, *8*, 9511−9517.

DOI: 10.1021/acsami.6b02156
ACS Appl. Mater. Interfaces 2016, 8, 10545−10550

(25) Putz, K. W.; Compton, O. C.; Palmeri, M. J.; Nguyen, S. T.; Brinson, L. C. High-Nanofiller-Content Graphene Oxide-Polymer Nanocomposites *via* Vacuum-Assisted Self-Assembly. *Adv. Funct. Mater.* **2010**, *20*, 3322−3329.
(26) Li, Y. Q.; Yu, T.; Yang, T. Y.; Zheng, L. X.; Liao, K. Bio-Inspired Nacre-Like Composite Films Based on Graphene with Superior Mechanical, Electrical, and Biocompatible Properties. *Adv. Mater.* **2012**, *24*, 3426−3431.
(27) Hu, K.; Tolentino, L. S.; Kulkarni, D. D.; Ye, C.; Kumar, S.; Tsukruk, V. V. Written-in Conductive Patterns on Robust Graphene Oxide Biopaper by Electrochemical Microstamping. *Angew. Chem., Int. Ed.* **2013**, *52*, 13784−13788.
(28) Park, S.; Lee, K.-S.; Bozoklu, G.; Cai, W.; Nguyen, S. T.; Ruoff, R. S. Graphene Oxide Papers Modified by Divalent Ions-Enhancing Mechanical Properties *via* Chemical Cross-Linking. *ACS Nano* **2008**, *2*, 572−578.
(29) Liu, R.-Y.; Xu, A.-W. Byssal Threads Inspired Ionic Cross-Linked Narce-Like Graphene Oxide Paper with Superior Mechanical Strength. *RSC Adv.* **2014**, *4*, 40390−40395.
(30) Ye, Y.-S.; Zeng, H.-X.; Wu, J.; Dong, L.-Y.; Zhu, J.-T.; Xue, Z.-G.; Zhou, X.-P.; Xie, X.-L.; Mai, Y.-W. Biocompatible Reduced Graphene Oxide Sheets with Superior Water Dispersibility Stabilized by Cellulose Nanocrystals and Their Polyethylene Oxide Composites. *Green Chem.* **2016**, *18*, 1674−1683.

DOI: 10.1021/acsami.6b02156
ACS Appl. Mater. Interfaces 2016, 8, 10545−10550